

# High Performance Evanescent Edge Coupled Waveguide Unitraveling-Carrier Photodiodes for >40-Gb/s Optical Receivers

M. Achouche, V. Magnin, J. Harari, F. Lelarge, E. Derouin, C. Jany, D. Carpentier, F. Blache, and D. Decoster

**Abstract**—We have demonstrated a low-cost high-bandwidth and high-responsivity evanescent waveguide untravelling-carrier photodiode (PD) fabricated using all 2-in InP processing including on-wafer mirrors and coating. Optimization of the optical input waveguide was made using the method of the genetic algorithm associated with a beam propagation method. Optical fiber coupling to the PD is based on a diluted multimode waveguide allowing simple material epitaxial growth. The fabricated PDs exhibit simultaneously 0.76-A/W responsivity at 1.55  $\mu\text{m}$ , >50-GHz bandwidth, and more than 22-mA average saturation photocurrent at 50 GHz. The light polarization dependence is less than 0.1 dB.

**Index Terms**—Genetic algorithms, multimode waveguides, optical fiber coupling, optical receivers, photodiodes (PDs).

## I. INTRODUCTION

**F**UTURE optical receivers for 40-Gb/s dense wavelength-division-multiplexing transmission systems require an optical preamplifier (OPA) using erbium-doped fiber amplifiers or semiconductor optical amplifiers [1] to improve the sensitivity. In such OPA receivers, the high output current of the photodiode (PD) can be directly fed into the decision circuit without using a transimpedance electrical amplifier. For example, in a high bit-rate time-division-multiplexing system, this new receiver scheme without electronic amplifiers is required for system simplicity and improved signal-to-noise ratio [2]. Such high-power PDs could ensure better phase margin and high robustness. High saturation power PDs are also suitable in millimeter/micro-wave optical fiber links.

Evanescent waveguide PD using a planar diluted multimode waveguide can provide high responsivity together with good power handling capabilities and large fiber alignment tolerances [3]. Evanescent coupling allows also progressive absorption of light allowing a better distribution of photogenerated carriers along the diode. However, in conventional PIN, PD output saturation occurs at moderate power and the high-speed response degrades at high power as a result of space charge effect due to photogenerated holes. Recently, untravelling-carrier PDs (UTC-PDs) have been proposed to relax the space charge effect

by using only electrons as active carriers to take advantage of their high velocity [4]. A UTC-PD with an edge-illuminated refracting-facet demonstrated promising performances [5]. The device we developed uses a planar diluted multimode waveguide without additional, usually costly, antireflection (AR) coating after cleaving. The processing simplicity of this design makes it suitable for the fabrication of 40-Gb/s low cost receivers.

In this letter, we report an evanescent waveguide UTC-PDs developed using a 2-in wafer process technology with dry etched mirror facets for on-wafer AR coating. Responsivity of 0.76 A/W with very low polarization dependence (0.1 dB) and wide coupling tolerances (2  $\mu\text{m}$  vertical and 5  $\mu\text{m}$  horizontal), bandwidth over 50-GHz and 22-mA average photocurrent at 50 GHz have been achieved.

## II. EVANESCENT UTC DESIGN AND FABRICATION

The epitaxial structure of the evanescent waveguide UTC-PD is grown using gas source molecular beam epitaxy on InP-Fe substrate. The structure comprises a p (few  $10^{17} \text{ cm}^{-3}$ ) InGaAs absorption layer (0.2  $\mu\text{m}$ ) inserted between a p+ InP barrier layer (0.5  $\mu\text{m}$ ) and a n- InGaAsP ( $\lambda = 1.3 \mu\text{m}$ ) collector layer (0.4  $\mu\text{m}$ ). A multimode diluted waveguide made from very thin quaternary layers inserted in InP is used to couple the light from the input facet to the absorber [6]. A quaternary matching layer is inserted between the waveguide and the collector to increase coupling efficiency [6].

The design of such a structure was performed using a genetic algorithm, a multiparameter optimization method to carry the numerous optimization parameters, coupled to a two-dimensional beam propagation method (BPM) simulation tool [6]. Further calculations have then been performed using three-dimensional BPM to take into account lateral divergence.

Fig. 1 shows the measured and simulated responsivity at 1.55- $\mu\text{m}$  wavelength for various optical input waveguide lengths, for a  $5 \times 25 \mu\text{m}^2$  area PD. The calculated responsivity follows a sinusoidal shape with 44- $\mu\text{m}$  period and reaches a maximum as high as 0.97 A/W for a waveguide length of 20  $\mu\text{m}$  with a polarization dependence below 0.1 dB. The position of the maximum measured responsivity (0.76 A/W) is very close to the theoretical results. However, slightly lower responsivities are measured on our UTC diodes, probably due to optical loss induced by roughness on the input facet.

The process flow of our evanescent waveguide PDs fabrication is mainly based on the dry etching process for mesa real-

Manuscript received August 21, 2003; revised October 1, 2003. This work was conducted in part under the French RNRT Project POPEYE.

M. Achouche, F. Lelarge, E. Derouin, C. Jany, D. Carpentier, and F. Blache are with the ALCATEL Research and Innovation, 91461 Marcoussis, France (e-mail: mohand.achouche@alcatel.fr).

V. Magnin, J. Harari, and D. Decoster are with the IEMN, 59652 Villeneuve d'Ascq, France.

Digital Object Identifier 10.1109/LPT.2003.821082

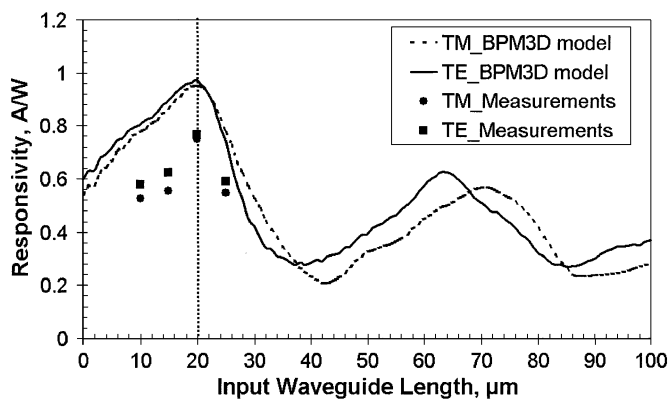


Fig. 1. Responsivity at 1.55- $\mu\text{m}$  wavelength of UTC versus optical input waveguide length.

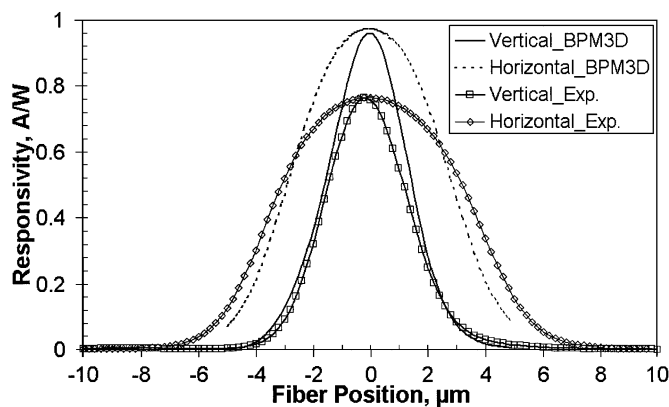


Fig. 3. Responsivity of a  $5 \times 25 \mu\text{m}^2$  UTC-PD with a  $20\text{-}\mu\text{m}$ -long input waveguide ( $\lambda = 1.55 \mu\text{m}$ ).

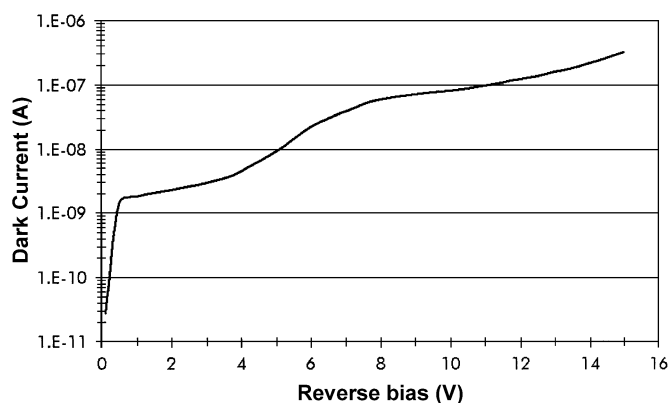


Fig. 2. Typical current–voltage ( $I$ – $V$ ) characteristics of an edge-coupled UTC diode.

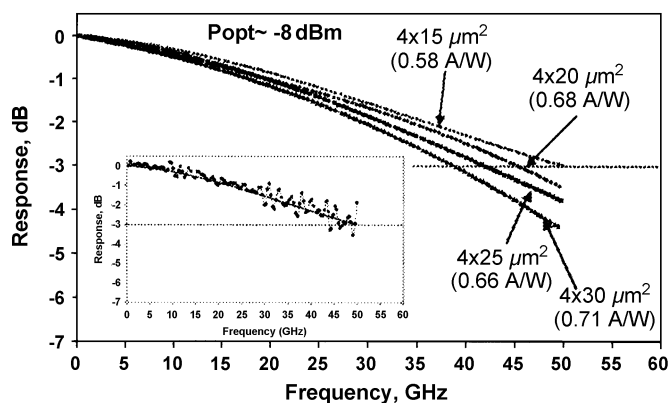


Fig. 4. Frequency response of  $4 \times 15$ ,  $4 \times 20$ ,  $4 \times 25$ , and  $4 \times 30 \mu\text{m}^2$  UTC, at low optical power and a  $-3\text{-V}$  bias (the insert figure shows the raw data and fitted response).

ization, device isolation, and waveguide input facet etching with AR coating deposition on wafer ( $\text{SiN}_x$  chemical vapor deposition also acting as a junction passivation layer). Fig. 2 shows a typical dark current versus bias voltage characteristics for a UTC diode. The dark current is  $5 \text{ nA}$  at the reverse voltage of  $3 \text{ V}$  and is less than  $100 \text{ nA}$  up to  $10 \text{ V}$ , where the tunneling current becomes dominant. This low dark current indicates the good passivation process of the mesa junction. Moreover, passivation of the input facet in evanescent coupling detectors is not an issue since it is not electrically active as it is the case for direct illumination detectors where lateral expansion of the depletion region might reach the input facet.

Typical series resistances and capacitances extracted from S11 up to  $65 \text{ GHz}$  at a reverse bias of  $3 \text{ V}$  are  $8 \Omega$  and  $42 \text{ fF}$  for a PD of  $4 \times 25 \mu\text{m}^2$  junction area, respectively. Even for a  $4 \times 15 \mu\text{m}^2$  UTC, the series resistance is as low as  $11 \Omega$  and the associated junction capacitance is  $28.5 \text{ fF}$ . These low values ensure a small contribution of the resistance–capacitance time constant to the PD bandwidth.

### III. DEVICE CHARACTERISTICS

Fig. 3 shows responsivity tolerance measurements at  $1.55\text{-}\mu\text{m}$  wavelength for a  $5 \times 25 \mu\text{m}^2$  PD with a  $20\text{-}\mu\text{m}$ -long input waveguide coupled with a  $4\text{-}\mu\text{m}$ -mode diameter lensed fiber. Responsivity is  $0.76 \text{ A/W}$  with almost no bias dependence and limited

polarization sensitivity ( $0.1 \text{ dB}$ ). These performances are maintained over the whole  $C$ -band. The measured misalignment tolerances at  $-1 \text{ dB}$  are  $5$  and  $2 \mu\text{m}$  for the horizontal and vertical directions, respectively, which are very close to simulation results, reducing the complexity of the pigtailling process to ensure a photoreceiver module at affordable cost.

Fig. 4 shows the output power frequency response (decibels) of UTC-PDs with  $4\text{-}\mu\text{m}$  width and  $15\text{-}$ ,  $20\text{-}$ ,  $25\text{-}$ , and  $30\text{-}\mu\text{m}$  length, respectively, using a heterodyne setup and a low optical power to achieve a constant photocurrent of  $0.1 \text{ mA}$  on a  $50\text{-}\Omega$  load and a  $3\text{-V}$  reverse bias (the insert on Fig. 4 shows the raw data and fitted response). The  $-3\text{-dB}$  bandwidth of the  $4 \times 30 \mu\text{m}^2$  UTC is  $39 \text{ GHz}$ , whereas, it reaches  $50 \text{ GHz}$  for the  $4 \times 15 \mu\text{m}^2$  UTC. Worst noting is the high bandwidth obtained under low optical power injection ( $\sim -8 \text{ dBm}$ ) due to a low p-absorption layer doping level and an optimized absorption–collector interface to efficiently transfer electrons to the collector layer. Measurements of the frequency response under high optical power injection of  $+10 \text{ dBm}$  (Fig. 5) demonstrate bandwidth in excess of  $50 \text{ GHz}$  whatever the PD length. We measure less than  $1.4\text{-dB}$  loss on a UTC of  $4 \times 15 \mu\text{m}^2$  ( $0.65 \text{ A/W}$ ). The bandwidth improvement under high optical power injection is associated to a change of the collector charge state due to electrons injection in the absorber–collector (AC) junction:

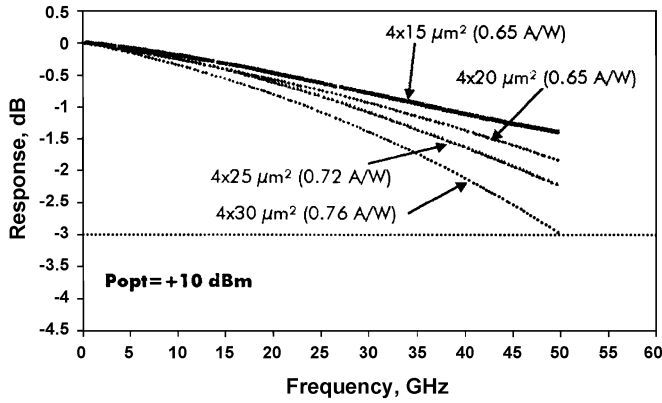


Fig. 5. Frequency response of  $4 \times 15$ ,  $4 \times 20$ ,  $4 \times 25$ , and  $4 \times 30 \mu\text{m}^2$  UTC, at  $+10$ -dBm optical power and a  $-3$ -V bias.

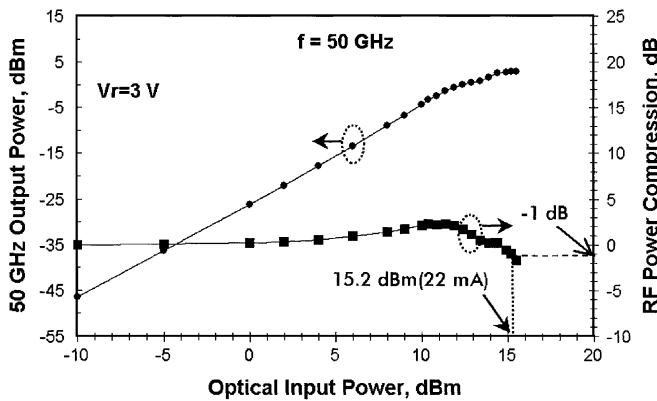


Fig. 6. 50-GHz output power and RF power compression of UTC ( $4 \times 25 \mu\text{m}^2$ ) at a bias of  $-3$ -V versus optical input power.

- Transit time reduction by current injection: the electrical field is reduced at the collector input and reinforced at the output (modification of the electrical field slope).
- Reduction of the AC capacitance: the total capacitance is reduced due to subtraction of the differential capacitance  $I_C \times (d\tau_C/dV_{AC})|_{W_C}$ , proportional to the current, from the depletion capacitance, as long as the high injection effects are not occurring.

Responsivity improvement with optical power level suggests a reduced recombination in the p-absorption layer to be the origin.

The measured output power at 50 GHz and the radio-frequency (RF) power compression at a reverse bias voltage of 3 V are plotted in Fig. 6 against the optical input power. More than 22-mA average photocurrent at 50 GHz ( $-1$ -dB compression) was extracted from the UTC corresponding to an optical

input power of 15.2 dBm with a very good linearity of the RF output power versus optical input power. This demonstrates that our high performance UTC-PD can directly supply an output voltage over 1 V, which is large enough to drive a  $D$  flip-flop in a 40-Gb/s optical receiver.

#### IV. CONCLUSION

In this letter, we have reported a new InGaAsP-InGaAs evanescent waveguide UTC-PDs with an original diluted optical waveguide design developed using a 2-in wafer processing which includes on-wafer AR coating. The devices exhibit state of the art performances: high responsivities (0.76 A/W) with low polarization dependence ( $<0.1$  dB) and large alignment tolerances as needed for cost-effective receivers packaging. High-speed operation of our UTC-PDs with bandwidth in excess of 50 GHz at both low and high optical power (up to 22 mA) demonstrates the capability for 40-Gb/s operation. These performances and simple manufacturing confirm the application potential for low cost and/or high performance 40-Gb/s receivers.

#### ACKNOWLEDGMENT

The authors thank S. Demiguel, L. Giraudet, and A. Scavennec for interesting discussions.

#### REFERENCES

- [1] E. Legros, T. Barrou, S. Vuye, L. Giraudet, C. Joly, F. Blache, T. Ducellier, and M. Goix, "High sensitivity high gain SOA-Filter-PIN-PHEMT 40-Gb/s photoreceiver," in *Proc. Eur. Conf. Optical Communications (ECOC'98)*, 1998, pp. 69–70.
- [2] K. Hagimoto, Y. Miyamoto, T. Kataoka, H. Ichino, and O. Nakajima, "Twenty-Gbit/s signal transmission using simple high sensitivity optical receiver," in *Proc. Optical Fiber Communications (OFC'92)*, 1992, pp. 48–49.
- [3] M. Achouche, S. Demiguel, E. Derouin, D. Carpentier, F. Barthe, F. Blache, V. Magnin, J. Harari, and D. Decoster, "New all 2-inch manufacturable high performance evanescent coupled waveguide photodiodes with etched mirrors for 40 Gb/s optical receivers," in *Proc. Optical Fiber Communications (OFC 2003)*, 2003, pp. 23–24.
- [4] Y. Muramoto, K. Kato, M. Mitsuhashi, O. Nakajima, Y. Matsuoka, N. Shimizu, and T. Ishibashi, "High output voltage, high speed, high efficiency uni-travelling carrier waveguide photodiode," *Electron. Lett.*, vol. 34, no. 1, pp. 122–123, 1998.
- [5] Y. Muramoto, H. Fukano, T. Furuta, and Y. Matsuoka, "A polarization independent high efficiency refracting facet uni travelling carrier photodiode with a bandwidth over 50 GHz," in *Proc. Eur. Conf. Optical Communications (ECOC 2000)*, 2000, pp. 109–110.
- [6] V. Magnin, L. Giraudet, J. Harari, J. Decobert, P. Pagnot, E. Boucherez, and D. Decoster, "Design, optimization, and fabrication of side illuminated p-i-n photodetectors with high responsivity and high alignment tolerances for 1.3- and 1.55  $\mu\text{m}$  wavelength use," *J. Lightwave Technol.*, vol. 20, pp. 477–488, Mar. 2002.